Changing Dendritic Field Size of Mouse Retinal Ganglion Cells in Early Postnatal Development

Lei Ren,[1]* Haitian Liang,[1]* Ling Diao,[2]* Shigang He[1]

[1] Chinese Academy of Sciences, Institute of Biophysics, State Key Laboratory of Brain and Cognitive Sciences, Beijing 100101, China

[2] Institute of Neuroscience, Shanghai Institutes for Biological Sciences, Chinese Academy of Sciences, Shanghai 200031, China

Received 26 August 2009; revised 23 November 2009; accepted 2 December 2009

ABSTRACT: **During early postnatal development, dendrites of retinal ganglion cells (RGCs) extend and branch in the inner plexiform layer to establish the adult level of stratification, pattern of branching, and coverage. Many studies have described the branching patterns, transient features, and regulatory factors of stratification of the RGCs. The rate of RGC dendritic field (DF) expansion relative to the growing retina has not been systematically investigated. In this study, we used two methods to examine the relative expansion of RGC DFs. First, we measured the size of RGC DFs and the diameters of the eyeballs at several postnatal stages. We compared the measurements with the RGC DF sizes calculated from difference of the eyeball sizes based on a linear expansion assumption. Second, we used the number of cholinergic amacrine cells (SACs) circumscribed by the DFs of RGCs at corresponding time points as an internal ruler to assess the size of DFs. We found most RGCs exhibit a phase of faster expansion relative to the retina between postnatal day 8 (P8) and P13, followed by a phase of retraction between P13 and adulthood. The morphological α cells showed the faster growing phase but not the retraction phase, whereas the morphological ON–OFF direction selective ganglion cells expanded in the same pace as the growing retina. These findings indicate different RGCs show different modes of growth, whereas most subtypes exhibit a fast expansion followed by a retraction phase to reach the adult size.** © 2009 Wiley Periodicals, Inc. Develop Neurobiol 70: 397–407, 2010

Keywords: **retinal ganglion cells; dendritic fields; development; starburst cells; VAChT**

INTRODUCTION

Retinal ganglion cells (RGCs) are the output units of the eye, conveying information processed by the retina to the higher visual centers. Each subpopulation of RGCs extracts a certain aspect from the visual scene by forming specific neural circuitry with bipolar cells and amacrine cells. More than 10 types of cone bipolar cells innervate the inner plexiform layer (IPL) (Euler and Wassle, 1995; Chan et al., 2001; Wassle et al., 2009), whereas the rod bipolar cells piggyback their outputs on the cone pathways (Famiglietti and Kolb, 1975; DeVries and Baylor, 1995; Wassle, 2004). Most adult RGCs narrowly stratify in one or two of the 10 sublaminae in the IPL, where they interact with limited types of bipolar cells. The complexity in retinal processing most likely originates from the interaction with amacrine cells. Some 30 types of amacrine cells reside in the retina and innervate the IPL (Mariani, 1990; Wassle and Boycott, 1991; MacNeil and Masland, 1998;

*These authors contributed equally to this work.

Correspondence to: S. He (shiganghe@moon.ibp.ac.cn).

Contract grant sponsor: NSFC Key Project Grant; contract grant number: 30530280.

Contract grant sponsor: National Basic Research Program of China; contract grant numbers: 2007CB512208 and 2006CB911003.

Published online 7 December 2009 in Wiley InterScience (www.interscience.wiley.com).
DOI 10.1002/dneu.20777

MacNeil et al., 1999; Lin and Masland, 2006), interact with bipolar and ganglion cells, therefore form the basis for complicated processing of visual information in the retina.

The RGCs and amacrine cells are among the earliest retinal neurons to differentiate (Young, 1985a,b; Cepko et al., 1996; Rapaport et al., 2004) and begin to form conventional synapses with each other from postnatal day 3 (P3) in the mouse retina (Olney, 1968; McArdle et al., 1977; Fisher, 1979). It has been shown that a certain percentage of RGCs exhibit adult-like light responses at eye opening (Bowe-Anders et al., 1975; Masland, 1977; Dacheux and Miller, 1981). For the subtype of RGCs coding motion directions, adult-like ability to detect motion directions emerge at the onset of RGCs' light sensitivity (Chen et al., 2008), indicating the formation of circuitry for processing motion directions is likely complete before the reception of light driven inputs from bipolar cells. The completely light independent maturation of the circuitry further supports this speculation (Chan and Chiao, 2008; Chen et al., 2008; Elstrott et al., 2008).

However, the circuitries connected in early postnatal stage need to deal with one important change, namely, the expansion of the retina. If the rate of RGC dendrite extension is different from interstitial stretch, rewiring is required to maintain the neural circuitries. Many studies in the literature examined the developmental changes of the RGCs including transient features, dendritic remodeling, stratification, and interaction in many species (Perry and Linden, 1982; Leventhal et al., 1988; Ramoa et al., 1988; Yamasaki and Ramoa, 1993; Weber et al., 1998; Wong et al., 2000; Wong and Wong, 2001; Yamagata et al., 2002; Lin et al., 2004; Mumm et al., 2005; Xu and Tian, 2007; Tian, 2008; Yamagata and Sanes, 2008). To our knowledge, the only attempt in the literature to evaluate differential change of the ganglion cell density is in the rabbit retina using Müller cells as a reference (Reichenbach et al., 1993; Deich et al., 1994).

On the basis of our previous work documenting development of RGCs in the mouse, we were able to estimate the size of DFs of RGCs at a particular stage from their size at an earlier stage and the difference of the eye ball size, assuming that RGCs expand linearly with the retina. The estimation from the entire sample population showed that RGCs exhibited a phase of interstitial expansion (P0 to P8), followed by a phase of rapid growth, exceeding the pace of growing retina (P8 to P13), and finally a phase of retraction (P13 to adult). A subtype-by-subtype analysis revealed that only two subtypes of RGCs are different: α-cells do not exhibit the final retraction and the direction selective ganglion cells always expand in the same pace with the growing retina. To verify these findings, we used the mosaic of cholinergic amacrine cells (SACs) as an internal ruler to measure the changing size of RGCs relative to the expanding retina. The measurements confirmed the calculation at every stage and for every subtype examined. Our results indicate that DFs of most RGCs exhibit a phase of interstitial stretching, followed by a phase of rapid expansion exceeding the rate of growing retina, and then a phase of retraction. Given that many RGCs showed adult-like light responses at eye opening (Bowe-Anders et al., 1975; Masland, 1977; Dacheux and Miller, 1981), these findings suggest that the retinal circuitries formed in early postnatal stages undergo substantial rewiring processes.

METHODS

Isolated Retinal Preparation

The procedures of using and handling animals conform to the institutional guidelines of the Institute of Biophysics, Chinese Academy of Sciences and to the ARVO statement for the Use of Animals in Ophthalmic and Vision Research. C57BL/6N mice or transgenic mice expressing yellow fluorescent protein (YFP[H] line, The Jackson Laboratory) at various postnatal days were anesthetized by hypothermia or ether, the eyes quickly enucleated, and the animals sacrificed. Horizontal and vertical diameters of the eye balls were measured using a vernier caliper and recorded for later estimation of DF size of RGCs. Then a slit was cut in the sclera close to the cornea. The eyes were submerged in oxygenated Ames medium and the retina carefully isolated from the pigment epithelium. The dissection was carried out using a Nikon SMZ660 dissection stereo microscope. The isolated retinas were incubated in oxygenated Ames solution containing 1 μg/mL 4,6-diamidino-2-phenynolindole (DAPI, Sigma D9542), being constantly bubbled with 95% O_2 and 5% CO_2 for 1 h to stain somata of all cells. The retina was fixed with 4% paraformaldehyde for 45 min, rinsed three times in 0.1*M* phosphate buffer (PB; pH 7.4) and was ready for histochemiscal labeling.

Gene Gun Labeling

The gene gun process was described in detail by Sun et al. (2002). Briefly, 2 mg of 1,1′-dioctadecyl-3,3,3′,3′-tetramethylindocarbocyanine perchlorate (DiI, Molecular Probes, N-22880) were dissolved in 200 μL of methylene chloride, mixed with 20 mg of tungsten particles ($\cong$1.6 μm in diameter, BioRad, 165-2269), then dropped onto a piece of ice. When methylene chloride evaporated completely, DiI was

coated onto tungsten particles. After ice thawed out, we collected the suspension in a test tube and sonicated the particles for 5 min to prevent the formation of large clusters. Lengths of Tefzel tubing (up to 76 cm) were loaded with DiI-tungsten microcarrier complexes using the tubing prep station (BioRad, 165-2420). Coated tubing was cut into 1.25 cm cartridges using the tubing cutter (BioRad, 165-2422). The DiI-coated tungsten particles were propelled into the whole-mount retina prelabeled with antibodies against choline acetyltransferase (anti-ChAT; Chemicon, Temecula, CA) using a BioRad Helios Gene Gun System (BioRad, 165-2432) with the helium pressure set at 300 psi. We inserted two layers of nylon net filter with the pore size of 30 μm (Millipore, NY3002500) between accelerator channel cone and retinal preparation to block the clusters of tungsten particles not separated completely in previous steps. Once the tungsten particles contacted the RGCs, DiI diffused along the membrane and labeled the entire cell. The preparation was then mounted on a slide with 0.1*M* PB and sealed with nail polish.

Immunohistochemistry

To enhance the YFP signal and to stain SACs, fixed retinas were incubated in a mixture of a rabbit polyclonal antibody against GFP (1:100; Chemicon, Temecula, CA) and a goat polyclonal antibody against choline acetyltransferase (1:100; anti-ChAT, Chemicon, Temecula, CA) for 3 days with 0.5% TritonX-100 and 1% Bovine Serum Albumin (BSA) at 4°C. Retinas were then rinsed three times with 0.01*M* PBS and incubated in the secondary antibodies (FITC-conjugated Donkey anti-rabbit 1:100, TRITC-conjugated Donkey anti-goat 1:200, Jackson ImmunoResearch Laboratories, Inc., West Grove, PA) with 0.2% tritonX-100 and 1% BSA overnight at 4°C. Negative controls were carried out by omitting primary antibodies. Retinas were flattened, mounted on glass slides with Vectashield (Vector Laboratories, Burlingame, CA) to retard fading.

In an attempt to label all proliferating cells, P8 mouse received two injections of 5% Bromodeoxyuridine (BrdU, Sigma) intraperitoneally (50 mg/kg) at an interval of 12 h (Young, 1985a,b; Alexiades and Cepko, 1996; Rachel et al., 2002), observations were made at P20. Tissue was treated with 2*N* HCl and 1% Triton X-100 for 2 h at 37°C to denature the DNA. After 1 h rinse in 0.1*M* borate, blocking solution was added for 15 min (5% normal goat serum; Sigma). Tissue was incubated in monoclonal mouse anti-BrdU (1:100; Sigma) and rabbit anti-ChAT (1:100; Chemicon, Temecula, CA) for 4 days at 4°C and in secondary antibodies (FITC-conjugated Goat anti-mouse 1:100, TRITC-conjugated Goat anti-rabbit 1:200; Jackson ImmunoResearch Laboratories, Inc., West Grove, PA) overnight at 4°C.

To examine SACs apoptosis at P8, immunostaining was combined with TDT (terminal deoxynucleotidyl transferase)-mediated dUTP nick end labeling (TUNEL) technique. Briefly, retinas were fixed for 5 h in fresh 3.7% formaldehyde. The fixative should be changed at least once after the first hour. After washing with 0.01*M* PB (pH 7.4), the tissue was permeated with 5% Triton X-100 for 1 day at 4°C, then processed for a TUNEL assay with TACS^{TM} TDT Kit (R&D Systems, Inc.) following the manufacturer's instructions. After TDT labeling, the tissue was incubated in 1:100 Goat anti-ChAT primary antibody (Chemicon, Temecula, CA) for 2 days at 4°C, then transferred to secondary antibody (TRITC-conjugated Donkey anti-Goat 1:200; Jackson ImmunoResearch Laboratories, Inc., West Grove, PA) and streptavidin-fluorescein (1:100; R&D Systems, Inc.) at 4°C overnight. We also performed TACS-Nuclease treated positive control to generate DNA breaks in a majority of cells.

Data Analysis

Images of RGCs were collected using a Nikon ECLIPSE E800 microscope equipped with a Photometrics Cascade 512B camera (Roper Scientific, Inc.). Most images were collected with a Nikon Plan Apo oil 40× [numerical aperture (NA) 1.0] objective; for large cells, a Nikon Plan Apo 20× (NA 0.75) objective was used to show the entire DF. Some double-labeled specimens were visualized with an OLYMPUS-FV500 confocal laser-scanning microscope. Images were acquired using a 20× and a 40× objective lens with a resolution of 1024 × 1024 pixels. The brightness and contrast of all images were reversed using Adobe Photoshop 8.0 to give a better illustration of the DF. As the center of highest ganglion cell density is located quite near the optic disk (Drager and Olsen, 1981; Jeon and Masland, 1995), the distance of the cell to the center of the optic nerve head was measured and taken as the cell's eccentricity. The DAPI labeled somas were used to estimate the dendritic stratification of ganglion cells in the IPL. The level of stratification was defined as 0–100% from the border of the inner nuclear layer to the border of the ganglion cell layer and measured by taking the *z*-axis reading on the Nikon ECLIPSE E800 microscope. The dendritic branching pattern was assessed independently by three experienced observers and the results compared. For those in dispute, a discussion was held until a consensus reached.

To quantify DF size, a convex polygon was drawn by linking the outermost tips of dendrites, and the area calculated using a graphic program MetaMorph 4.5 (Universal Imaging). The area was converted to diameter by assuming a circular DF. Based on an assumption that DF expand linearly with the retina and also the eye ball, the diameter of DF at particular stage can be calculated from the ratio of diameter of the eye balls between two stages and DF size of the earlier stage as following formula:

$$\mathrm{DF}_{\mathrm{prdt}} = \frac{D_{\mathrm{L}}}{D_{\mathrm{E}}} \times \mathrm{DF}_{\mathrm{E}},$$

where D_{E} and DF_{E} are the diameters of the eye balls and DFs at an earlier postnatal day, respectively, D_{L} is the diameter of the eye balls at a later stage, and $\mathrm{DF}_{\mathrm{prdt}}$ is DF size predicted from the ratio of eyeball diameters and the diameter of DFs at an earlier stage. The reason to calculate

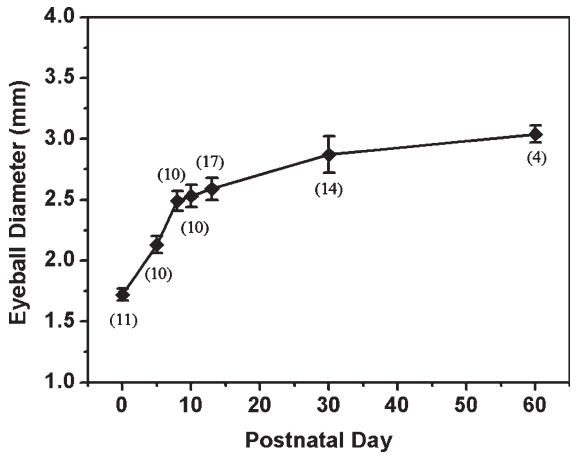

Figure 1 Changing eye ball size. The diameters of the eye balls are plotted against the age of the animals, mean ± SD.

the diameter is that it is the same as to calculate area as shown blow:

$$\pi r_{\mathrm{prdt}}^2 = \frac{4\pi R_{\mathrm{L}}^2}{4\pi R_{\mathrm{E}}^2} \times \pi r_{\mathrm{E}}^2, \quad (1)$$

$$r_{\mathrm{prdt}} = \frac{R_{\mathrm{L}}}{R_{\mathrm{E}}} \times r_{\mathrm{E}}, \quad (2)$$

$$\mathrm{DF}_{\mathrm{prdt}} = \frac{D_{\mathrm{L}}}{D_{\mathrm{E}}} \times \mathrm{DF}_{\mathrm{E}}, \quad (3)$$

where R_{E} and R_{L} are the radius of the eye balls at an earlier and later stages, respectively, and r_{prdt} and r_{E} are the radius of predicted DF and measured DF at the earlier stage, respectively.

When we compared the densities of the SACs at different developmental stages, we sampled 12 regions along the vertical and horizontal meridians at 1/4, 1/2, 3/4 radius from the optic nerve head to the edge of the retina. When we used the mosaic of SACs to evaluate the relative changing size of RGCs, we counted the number of SACs circumscribed by the convex polygon linking the outmost tips of dendrites of RGCs. Statistical analyses were performed on raw data with Origin 8.0, and Mann-Whitney test was used on data not normally distributed or two sample *t*-test was used for comparison of data following normal distribution. Statistical significance was established as $p < 0.05$ or $p < 0.01$.

RESULTS

We measured the eyeball diameters at the same time points as we sampled the RGCs dendritic morphology, i.e., at P0, P8, P13, and adult (>P30). The eyeballs grow from 1.72 ± 0.06 mm at P0 to 3.04 ± 0.06 mm in adult. There is very little individual variation in eyeball size (Fig. 1).

If DFs of RGCs expand linearly with the growing retina and also the growing eyeball, the size of DF at a later stage can be calculated from the ratio of diameters of the eyeballs between two stages and the DF size at the earlier stage (see Methods section). Using data published in our previous study (Diao et al., 2004) and 507 RGCs acquired in this study, we calculated the DF size of the RGCs and compared the estimations with the measurements. It is clear that the growth of the RGC DFs undergoes different phases during early postnatal development (Fig. 2). From P0 to P8, the estimations matched the measurements indicating that the increase in DF can be almost completely accounted for by interstitial stretching. From P8 to P13, the calculations significantly underestimated the size of DFs indicating that the interstitial stretching alone was not sufficient to account for the growth of the RGCs and the RGCs expanded more rapidly than the expanding retina. From P13 to adulthood, the same calculation overestimated the size of DFs suggesting that the RGCs underwent a retraction process reducing the size of DFs to counteract the interstitial stretching.

As we reported previously, P0 RGCs cannot be classified using the criteria established in adult, but from P8 on a predominant proportion of RGCs can be classified (Diao et al., 2004). To make sure that the trend reflected in our estimation is not contaminated by noises of comparing different subtypes, we

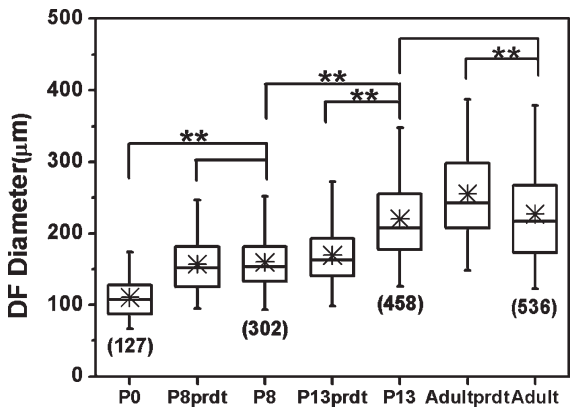

Figure 2 Box-graph showing difference in RGC dendritic diameters. Statistically significant differences are observed between every stage. P8prdt indicates size of dendritic fields predicted from the size of dendritic fields from P0 RGCs and the difference of size of the eye balls. The box and the whiskers indicate the quartiles and a range of 5–95%, respectively. The horizontal bar and the star symbol in each box indicate median and mean. $^{**}p < 0.01$. Similar convention is used in following figures.

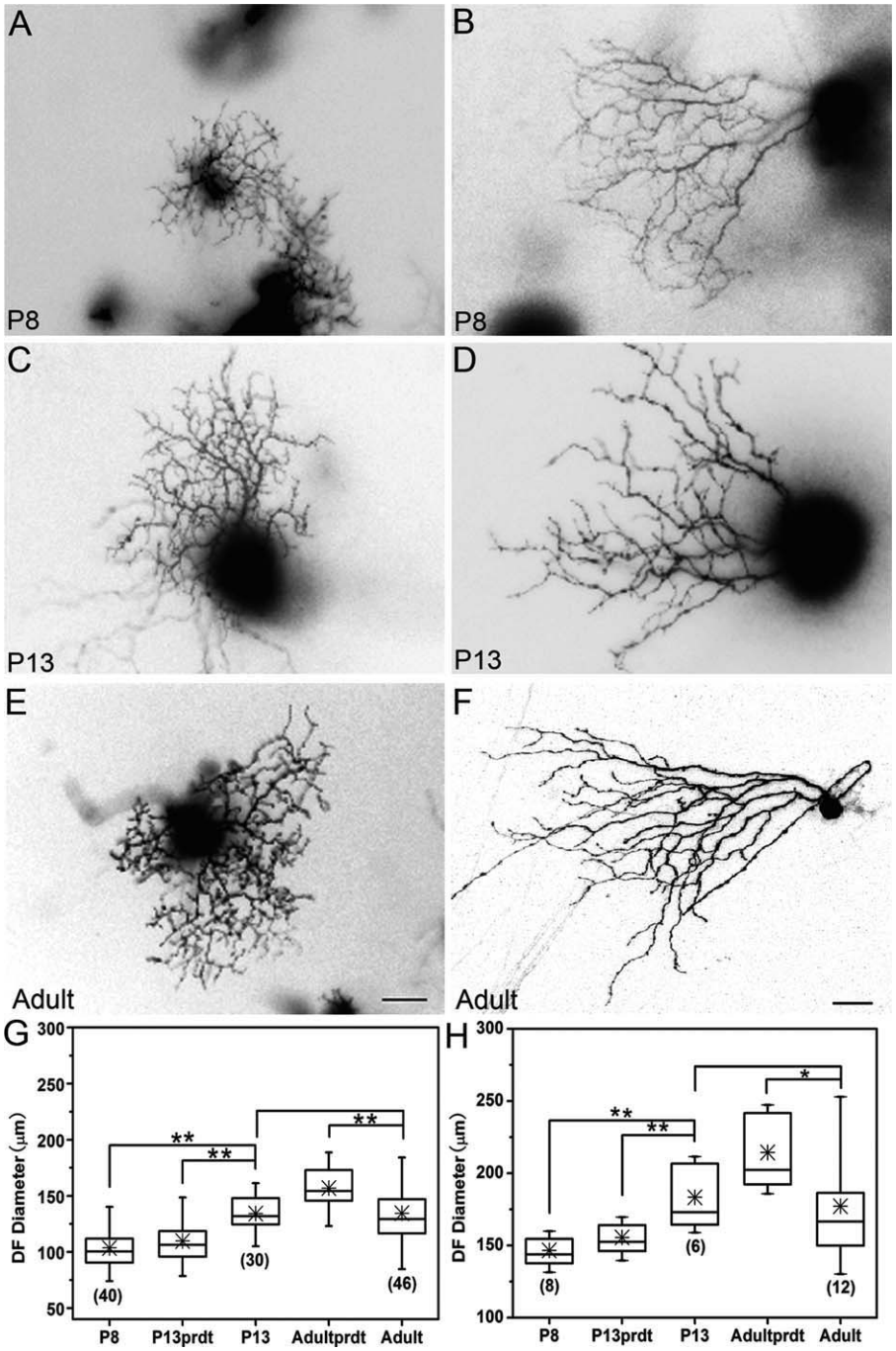

Figure 3 Over-expansion and retraction are also present when comparisons are made in the same subtype. A, C, E: Dendritic morphology of the RG_{B2} at P8, P13, and adult. G: Comparison of dendritic field size. B, D, F: Dendritic morphology of the RG_{C6} at P8, P13, and adult. H: Comparison of dendritic field size. Scale bar: 20 μm.

performed a subtype-by-subtype analysis. The results were consistent with the population comparison for subtypes RG_{A2}, RG_{B2}, RG_{B3}, RG_{B4}, RG_{C1}, RG_{C2}, RG_{C4}, RG_{C5}, and $RG_{C6.}$ Two examples are illustrated in Figure 3 for RG_{B2} and RG_{C6}. However, this more detailed analysis revealed some differences. The RG_{A1} cells showed a rapid expansion phase between P8 and P13 but no retraction after P13 [Fig. 4(A)], DFs of the RG_{D2} cells expanded with the expanding retina throughout our observation [Fig. 4(B)]. We did not have enough samples to yield any meaningful analysis for subtypes RG_{B1} and RG_{D1}.

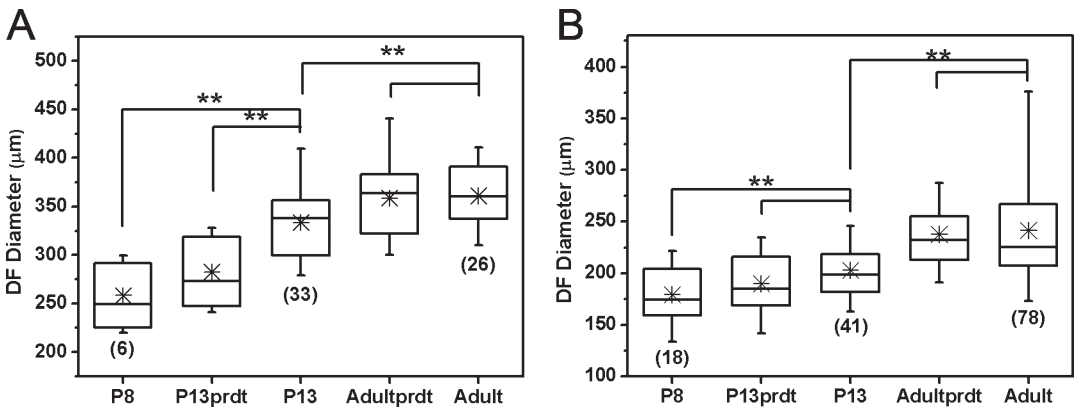

Figure 4 Two subtypes show different trends from the population comparison. A: RG_{A1} shows fast expansion between P8 and P13 but not retraction between P13 to adult. B: RG_{D2} always exhibit same pace of expansion as the retina.

To further verify these observations, we used the mosaic of SACs as an internal ruler to assess the changing size of RGC DFs relative to the growing retina. To do so, we need to first make sure that the number of SACs is not changing after P8. We performed a BrdU and a TUNEL labeling to examine if there are new SACs being generated or SACs undergoing apoptotic processes. No double labeled cells with cholinergic marker and BrdU [Fig. 5(A)] or TUNEL [Fig. 5(B)] were observed after P8 indicating that both proliferation and apoptotic processes of SACs were complete by P8. Second, we showed the decreasing density of SACs can be completely accounted for by interstitial growth from P8 to P13 and to adulthood (Fig. 6). Therefore, the number of SACs circumscribed by the DF of an RGC (Fig. 7) is expected to remain constant if the RGC DF only undergoes interstitial stretching. If the DF of an RGC expands faster than the growing retina, the number of SACs circumscribed by the RGC would increase, otherwise, if dendrites of a RGC retract, the number of circumscribed SACs would decrease. When we compared the number of SACs circumscribed by four types of RGCs (RG_{A1}, RG_{B2}, $RG_{C6,}$ and RG_{D2}) at different postnatal stages, the number of SACs circumscribed by RG_{B2} and RG_{C6} exhibited a significant increase from P8 to P13 and a significant decrease from P13 to adult [Fig. 8(A,B)], confirming the observations made from earlier calculations. Also consistent with the calculation, the number of SACs circumscribed by RG_{A1} significantly increased from P8 to P13, but remained unchanged after P13 [Fig. 8(C)]. The number of SACs circumscribed by the bistratified RG_{D2} cells remained unchanged

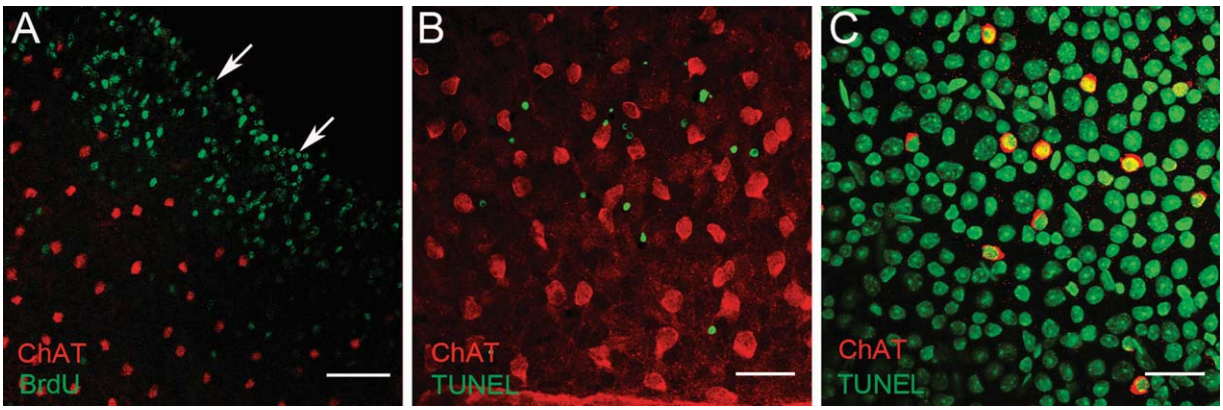

Figure 5 Stable population of cholinergic amacrine cells. A: BrdU labeling. BrdU positive cells are only observed in the far periphery of the retina, no double staining are observed with ChAT. B: No double staining of TUNEL in ChAT positive cells. C: Positive TUNEL control, showing after treating the retina with TACS-Nuclease, all cells, including ChAT positive cells can be stained by TUNEL. Scale bar: 50 μm in (A) and 25 μm in (B, C). [Color figure can be viewed in the online issue, which is available at www.interscience.wiley.com.]

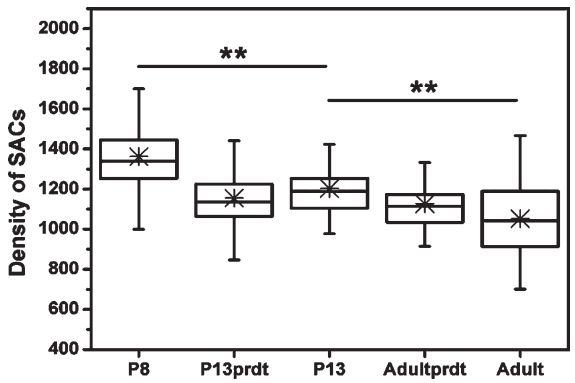

Figure 6 Changing density of cholinergic amacrine cells. The density of cholinergic amacrine cells are measured at P8, P13, and adult. The reduction in density can be completely accounted for by the expansion of the retina.

throughout these two stages indicating that this type of RGCs always grows in the same pace as the expanding retina [Fig. 8(D)].

Both the calculations based on the relationship of growing retina and growing DFs and the measurements made from changing number of SACs circumscribed by the RGC DFs showed that most subtypes of RGCs exhibited a fast growth followed by a retraction period. The morphological direction selective ganglion cells (RG_{D2}) expanded in the same pace with interstitial stretching. The alpha cells showed the faster growth phase from P8 to P13, but no retraction after P13.

DISCUSSION

Assumption of Uniform Expansion and Relative Expansion Rate

We estimated the changing size of DFs using an assumption of uniform expansion of the retina. This is not accurate in most mammalian species for two reasons. First, most mammalian retinas do not expand uniformly during early development, the peripheral retina expands much faster than the central retina (Mastronarde et al., 1984; Robinson et al., 1989). Second, most mammalian RGCs exhibit a clear difference in size of DF, the peripheral cells could be a few folds larger than the same type of cells in the central retina (Boycott and Wassle, 1974; Peichl et al., 1987; Wong, 1990; Dacey and Petersen, 1992; Milosevic et al., 2009), therefore, meaningful comparisons can only be made in the same eccentricity. However, in the mouse retina, the gradient of various cells is much smaller and density of various retinal neurons is much more uniform than most mammalian species (Jeon et al., 1998). The size of the RGCs is quite similar across the entire retina (Sun et al., 2002; Badea and Nathans, 2004). Therefore, the uniform assumption yields a more accurate estimate in the mouse than in most other mammalian species. Our measurements by counting the number of SACs circumscribed by RGC DFs showed that the uniform expansion assumption accurately predicted changing sizes of RGC DFs. The under- or overestimation by the uniform assumption is due to the different rate of extension of RGC dendrites relative to the retina rather than the nonuniform expansion of the retina.

The development of RGCs has been extensively studied in many species, and recently also in mice. The previous work examined many aspects of developing RGCs including cell proliferation and fate determination (Young, 1985a,b; Cepko et al., 1996; Rapaport et al., 2004), transient dendritic features (Ramoa et al., 1988; Yamasaki and Ramoa, 1993; Wong et al., 2000; Wong and Wong, 2001), stratification (Yamagata et al., 2002; Xu and Tian, 2007; Tian, 2008; Yamagata and Sanes, 2008), and interaction of dendrities of neighboring RGCs (Perry and Linden, 1982; Leventhal et al., 1988; Weber et al., 1998). However, the expansion rate of RGC DFs and mechanisms for dendritic tiling have not been systematically studied, although initial attempts have been

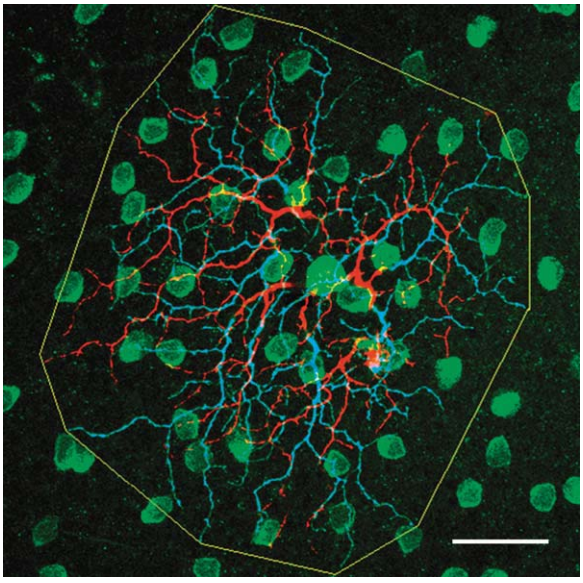

Figure 7 Measuring relative size. A GFP positive bistratified retinal ganglion cell is shown in red and blue (for ON and OFF stratifications), and cholinergic amacrine cells are shown in green. We counted the number of cholinergic amacrine cells circumscribed by the polygon linking outermost tips of dendrites. Scale bar: 25 μm. [Color figure can be viewed in the online issue, which is available at www.interscience.wiley.com.]

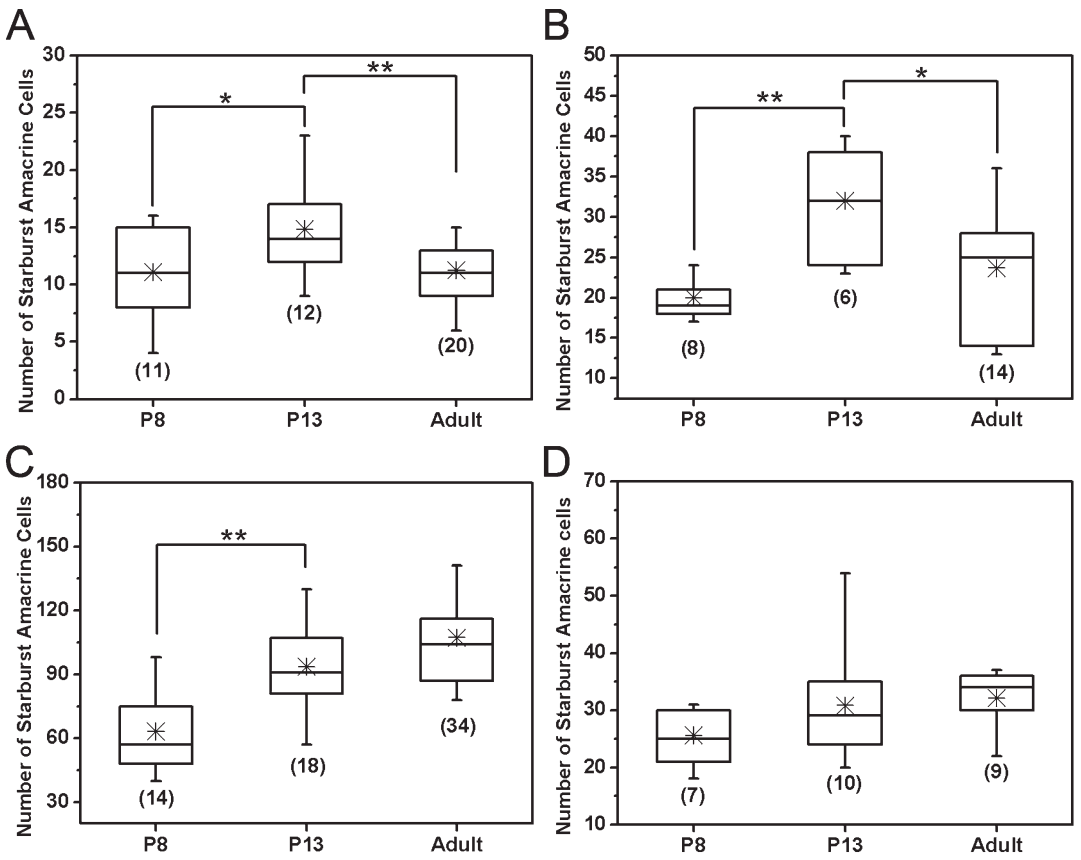

Figure 8 Relative expansion measured from changing number of cholinergic amacrine cells. A: Number of cholinergic amacrine cells circumscribed by RG_{B2}. B: Number of cholinergic amacrine cells circumscribed by RG_{C6}. Both (A) and (B) show significantly more cholinertic amacrine cells in P13 than in P8 and significantly fewer cholinergic amacrine cells in adult than P13. C: Number of cholinergic amacrine cells circumscribed by RG_{A1}. Significantly more cells are counted in P13 than in P8, but the number remains similar to P13 in adult. D: Number of cholinergic amacrine cells circumscribed by RG_{D2}. No statistically significant change in number of cells has been observed through development.

made in cat and rabbit (Dann et al., 1988; Wong, 1990; Ault and Leventhal, 1994; Deich et al., 1994).

In this study, we used the number of SACs to measure changing size of RGC DFs relative to the growing retina and used this method to verify the estimations we made from calculating sizes of eye balls and DFs. It turned out that all our estimations were confirmed by the measurements. The establishment of this reference system allows one to examine relative changes between the increasing DF size and growing retina, and can be applied to other cell types when necessary. The reference system does not need to be limited to cholinergic cells, as long as one can make sure the population is stable throughout the period of interest. This method would be particularly useful in species with a dramatically different expansion rate between central and peripheral retina because the reference cell population will smooth out the size difference and provide an accurate measure of the expanding retina.

Early work investigating differentiation of retinal cells showed that most amacrine cells are generated at E14–E18 (Cepko et al., 1996; Rapaport et al., 2004) and the massive apoptosis takes place from P3 to P8 (Young, 1984). In our study, we showed that from P8 on neither more SACs were generated nor were undergoing apoptotic processes. Therefore, the population of SACs is suitable for the purpose of evaluating differential changes between a subtype of neurons and the expanding retina.

Implications of Different Rate of Growth

Dendritic fields of a single population of sensory neurons completely cover the sensory surface with little

overlap, a phenomenon termed tiling. Dendritic tiling was first documented in cat RGCs (Wassle et al., 1981) and observed in species extending to fruit flies (Grueber et al., 2002) and nematodes worms (Gallegos and Bargmann, 2004). Recent work in invertebrates showed there are two modes to achieve tiling: a like-repel-like mode and a grow-and-retract mode. In the first case, the dendrites of the same cell or the same cell type repel each other, so they rarely cross or overlap (Emoto et al., 2004), and in the second case, the dendrites first overlap and then retract to achieve the final tiling pattern (Gallegos and Bargmann, 2004). Our data suggested that in the retina, these two modes to achieve dendritic tiling may coexist. Most RGCs may undergo a grow-and-retract mode and the direction selective ganglion cells may undergo a like-repel-like mode. The molecular mechanisms for dendritic tiling have been shown to relate to the function of Serine/Threonine Kinase pathway (Trc/Fry in Drosophila and Sax-1/Sax-2 in *C. elegans*) (Zallen et al., 2000; Tamaskovic et al., 2003; Emoto et al., 2004; Gallegos and Bargmann, 2004), it is not clear if the same mechanism is responsible for tiling of RGCs.

Depletion of the RGCs in a patch of retina causes neighboring RGCs to extend their dendrites into the depleted region (Perry and Linden, 1982; Hitchcock, 1989). Apparently, there is some recognition processes and stop signals because the filling-in dendrites would stop at some stage, presumably after contacting a certain number of dendrites originating from the same subtype of RGCs. However, faster expansion of the RGCs than the growing retina between P8 and P13 would result in increased contacts between neighboring cells of the same type. The stop signal is likely switched off during this period to allow the RGCs to occupy as much area as they can to compete for the inputs from bipolar cells (Deich et al., 1994; Maletic-Savatic et al., 1999). When the synaptogenesis stops, the dendrites that did not contact any bipolar cells would probably be pruned, resulting in a retraction of DF (Niell et al., 2004; Meyer and Smith, 2006; Cline and Haas, 2008).

Certain percentage of RGCs exhibit adult-like light responses at eye opening indicating the presence of adult-like neural circuitry (Bowe-Anders et al., 1975; Masland, 1977). The different expansion rate between RGC dendrites and retina would require the synapses between RGCs and bipolar cells or amacrine cells to turn over and rewire. However, the number of RGCs exhibiting a clear inhibitory surround increases during development indicating a maturation processes (Bowe-Anders et al., 1975; Masland, 1977), and dark-rearing changes the proportion of ON and OFF cells and synaptic inputs to the RGCs (Tian and Copenhagen, 2001, 2003). These findings are consistent with our results that the circuitry is still undergoing changes after eye opening. We recently demonstrated that the retinal circuitry coding motion directions emerge at P11, the onset of RGC light sensitivity (Chen et al., 2008). In this study, we found the direction selective ganglion cells always expand at the same rate of growing retina, possibly to avoid much turnover and rewiring.

The results described in this study illustrated a method to measure relative expansion of RGCs and would be interesting in understanding the mechanisms for RGC dendritic tiling and development of retinal circuitries.

The authors thank Yingye Zhang and Zhiping Liu for technical support.

REFERENCES

Alexiades MR, Cepko C. 1996. Quantitative analysis of proliferation and cell cycle length during development of the rat retina. Dev Dyn 205:293–307.

Ault SJ, Leventhal AG. 1994. Postnatal development of different classes of cat retinal ganglion cells. J Comp Neurol 339:106–116.

Badea TC, Nathans J. 2004. Quantitative analysis of neuronal morphologies in the mouse retina visualized by using a genetically directed reporter. J Comp Neurol 480:331–351.

Bowe-Anders C, Miller RF, Dacheux R. 1975. Developmental characteristics of receptive organization in the isolated retina-eyecup of the rabbit. Brain Res 87:61–65.

Boycott BB, Wassle H. 1974. The morphological types of ganglion cells of the domestic cat's retina. J Physiol 240: 397–419.

Cepko CL, Austin CP, Yang X, Alexiades M, Ezzeddine D. 1996. Cell fate determination in the vertebrate retina. Proc Natl Acad Sci USA 93:589–595.

Chan TL, Martin PR, Clunas N, Grunert U. 2001. Bipolar cell diversity in the primate retina: Morphologic and immunocytochemical analysis of a new world monkey, the marmoset *Callithrix jacchus*. J Comp Neurol 437: 219–239.

Chan YC, Chiao CC. 2008. Effect of visual experience on the maturation of ON-OFF direction selective ganglion cells in the rabbit retina. Vision Res 48:2466–2475.

Chen M, Weng S, Deng Q, Xu Z, He S. 2009. Physiological properties of direction-selective ganglion cells in early postnatal and adult mouse retina. J Physiol 587:819–828.

Cline H, Haas K. 2008. The regulation of dendritic arbor development and plasticity by glutamatergic synaptic input: A review of the synaptotrophic hypothesis. J Physiol 586:1509–1517.

Dacey DM, Petersen MR. 1992. Dendritic field size and morphology of midget and parasol ganglion cells of the human retina. Proc Natl Acad Sci USA 89:9666–9670.

Dacheux RF, Miller RF. 1981. An intracellular electrophysiological study of the ontogeny of functional synapses in the rabbit retina. II. Amacrine cells. J Comp Neurol 198: 327–334.

Dann JF, Buhl EH, Peichl L. 1988. Postnatal dendritic maturation of alpha and beta ganglion cells in cat retina. J Neurosci 8:1485–1499.

Deich C, Seifert B, Peichl L, Reichenbach A. 1994. Development of dendritic trees of rabbit retinal alpha ganglion cells: Relation to differential retinal growth. Vis Neurosci 11:979–988.

DeVries SH, Baylor DA. 1995. An alternative pathway for signal flow from rod photoreceptors to ganglion cells in mammalian retina. Proc Natl Acad Sci USA 92:10658–10662.

Diao L, Sun W, Deng Q, He S. 2004. Development of the mouse retina: emerging morphological diversity of the ganglion cells. J Neurobiol 61:236–249.

Drager UC, Olsen JF. 1981. Ganglion cell distribution in the retina of the mouse. Invest Ophthalmol Vis Sci 20: 285–293.

Elstrott J, Anishchenko A, Greschner M, Sher A, Litke AM, Chichilnisky EJ, Feller MB. 2008. Direction selectivity in the retina is established independent of visual experience and cholinergic retinal waves. Neuron 58: 499–506.

Emoto K, He Y, Ye B, Grueber WB, Adler PN, Jan LY, Jan YN. 2004. Control of dendritic branching and tiling by the Tricornered-kinase/Furry signaling pathway in *Drosophila* sensory neurons. Cell 119:245–256.

Euler T, Wassle H. 1995. Immunocytochemical identification of cone bipolar cells in the rat retina. J Comp Neurol 361:461–478.

Famiglietti EV Jr, Kolb H. 1975. A bistratified amacrine cell and synaptic cirucitry in the inner plexiform layer of the retina. Brain Res 84:293–300.

Fisher LJ. 1979. Development of synaptic arrays in the inner plexiform layer of neonatal mouse retina. J Comp Neurol 187:359–372.

Gallegos ME, Bargmann CI. 2004. Mechanosensory neurite termination and tiling depend on SAX-2 and the SAX-1 kinase. Neuron 44:239–249.

Grueber WB, Jan LY, Jan YN. 2002. Tiling of the *Drosophila* epidermis by multidendritic sensory neurons. Development 129:2867–2878.

Hitchcock PF. 1989. Exclusionary dendritic interactions in the retina of the goldfish. Development 106:589–598.

Jeon CJ, Masland RH. 1995. A population of wide-field bipolar cells in the rabbit's retina. J Comp Neurol 360: 403–412.

Jeon CJ, Strettoi E, Masland RH. 1998. The major cell populations of the mouse retina. J Neurosci 18:8936–8946.

Leventhal AG, Schall JD, Ault SJ. 1988. Extrinsic determinants of retinal ganglion cell structure in the cat. J Neurosci 8:2028–2038.

Lin B, Masland RH. 2006. Populations of wide-field amacrine cells in the mouse retina. J Comp Neurol 499:797–809.

Lin B, Wang SW, Masland RH. 2004. Retinal ganglion cell type, size, and spacing can be specified independent of homotypic dendritic contacts. Neuron 43:475–485.

MacNeil MA, Heussy JK, Dacheux RF, Raviola E, Masland RH. 1999. The shapes and numbers of amacrine cells: matching of photofilled with Golgi-stained cells in the rabbit retina and comparison with other mammalian species. J Comp Neurol 413:305–326.

MacNeil MA, Masland RH. 1998. Extreme diversity among amacrine cells: Implications for function. Neuron 20: 971–982.

Maletic-Savatic M, Malinow R, Svoboda K. 1999. Rapid dendritic morphogenesis in CA1 hippocampal dendrites induced by synaptic activity. Science 283:1923–1927.

Mariani AP. 1990. Amacrine cells of the rhesus monkey retina. J Comp Neurol 301:382–400.

Masland RH. 1977. Maturation of function in the developing rabbit retina. J Comp Neurol 175:275–286.

Mastronarde DN, Thibeault MA, Dubin MW. 1984. Non-uniform postnatal growth of the cat retina. J Comp Neurol 228:598–608.

McArdle CB, Dowling JE, Masland RH. 1977. Development of outer segments and synapses in the rabbit retina. J Comp Neurol 175:253–274.

Meyer MP, Smith SJ. 2006. Evidence from in vivo imaging that synaptogenesis guides the growth and branching of axonal arbors by two distinct mechanisms. J Neurosci 26:3604–3614.

Milosevic NT, Ristanovic D, Jelinek HF, Rajkovic K. 2009. Quantitative analysis of dendritic morphology of the alpha and delta retinal ganglion cells in the rat: A cell classification study. J Theor Biol 259:142–150.

Mumm JS, Godinho L, Morgan JL, Oakley DM, Schroeter EH, Wong RO. 2005. Laminar circuit formation in the vertebrate retina. Prog Brain Res 147:155–169.

Niell CM, Meyer MP, Smith SJ. 2004. In vivo imaging of synapse formation on a growing dendritic arbor. Nat Neurosci 7:254–260.

Olney JW. 1968. An electron microscopic study of synapse formation, receptor outer segment development, and other aspects of developing mouse retina. Invest Ophthalmol 7:250–268.

Peichl L, Ott H, Boycott BB. 1987. Alpha ganglion cells in mammalian retinae. Proc R Soc Lond B Biol Sci 231: 169–197.

Perry VH, Linden R. 1982. Evidence for dendritic competition in the developing retina. Nature 297:683–685.

Rachel RA, Dolen G, Hayes NL, Lu A, Erskine L, Nowakowski RS, Mason CA. 2002. Spatiotemporal features of early neuronogenesis differ in wild-type and albino mouse retina. J Neurosci 22:4249–4263.

Ramoa AS, Campbell G, Shatz CJ. 1988. Dendritic growth and remodeling of cat retinal ganglion cells during fetal and postnatal development. J Neurosci 8:4239–4261.

Rapaport DH, Wong LL, Wood ED, Yasumura D, LaVail MM. 2004. Timing and topography of cell genesis in the rat retina. J Comp Neurol 474:304–324.

Reichenbach A, Schnitzer J, Reichelt E, Osborne NN, Fritzsche B, Puls A, Richter U, Friedrich A, Knothe AK, Schober W, et al. 1993. Development of the rabbit retina. III: Differential retinal growth, and density of projection neurons and interneurons Vis Neurosci 10:479–498.

Robinson SR, Dreher B, McCall MJ. 1989. Nonuniform retinal expansion during the formation of the rabbit's visual streak: Implications for the ontogeny of mammalian retinal topography. Vis Neurosci 2:201–219.

Sun W, Li N, He S. 2002. Large-scale morphological survey of mouse retinal ganglion cells. J Comp Neurol 451: 115–126.

Tamaskovic R, Bichsel SJ, Hemmings BA. 2003. NDR family of AGC kinases–essential regulators of the cell cycle and morphogenesis. FEBS Lett 546:73–80.

Tian N. 2008. Synaptic activity, visual experience and the maturation of retinal synaptic circuitry. J Physiol 586: 4347–4355.

Tian N, Copenhagen DR. 2001. Visual deprivation alters development of synaptic function in inner retina after eye opening. Neuron 32:439–449.

Tian N, Copenhagen DR. 2003. Visual stimulation is required for refinement of ON and OFF pathways in postnatal retina. Neuron 39:85–96.

Wassle H. 2004. Parallel processing in the mammalian retina. Nat Rev Neurosci 5:747–757.

Wassle H, Boycott BB. 1991. Functional architecture of the mammalian retina. Physiol Rev 71:447–480.

Wassle H, Peichl L, Boycott BB. 1981. Dendritic territories of cat retinal ganglion cells. Nature 292:344–345.

Wassle H, Puller C, Muller F, Haverkamp S. 2009. Cone contacts, mosaics, and territories of bipolar cells in the mouse retina. J Neurosci 29:106–117.

Weber AJ, Kalil RE, Stanford LR. 1998. Dendritic field development of retinal ganglion cells in the cat following neonatal damage to visual cortex: Evidence for cell class specific interactions. J Comp Neurol 390:470–480.

Wong RO. 1990. Differential growth and remodelling of ganglion cell dendrites in the postnatal rabbit retina. J Comp Neurol 294:109–132.

Wong WT, Faulkner-Jones BE, Sanes JR, Wong RO. 2000. Rapid dendritic remodeling in the developing retina: Dependence on neurotransmission and reciprocal regulation by Rac and Rho. J Neurosci 20:5024–5036.

Wong WT, Wong RO. 2001. Changing specificity of neurotransmitter regulation of rapid dendritic remodeling during synaptogenesis. Nat Neurosci 4:351–352.

Xu HP, Tian N. 2007. Retinal ganglion cell dendrites undergo a visual activity-dependent redistribution after eye opening. J Comp Neurol 503:244–259.

Yamagata M, Sanes JR. 2008. Dscam and Sidekick proteins direct lamina-specific synaptic connections in vertebrate retina. Nature 451:465–469.

Yamagata M, Weiner JA, Sanes JR. 2002. Sidekicks: Synaptic adhesion molecules that promote lamina-specific connectivity in the retina. Cell 110:649–660.

Yamasaki EN, Ramoa AS. 1993. Dendritic remodelling of retinal ganglion cells during development of the rat. J Comp Neurol 329:277–289.

Young RW. 1984. Cell death during differentiation of the retina in the mouse. J Comp Neurol 229:362–373.

Young RW. 1985a. Cell differentiation in the retina of the mouse. Anat Rec 212:199–205.

Young RW. 1985b. Cell proliferation during postnatal development of the retina in the mouse. Brain Res 353: 229–239.

Zallen JA, Peckol EL, Tobin DM, Bargmann CI. 2000. Neuronal cell shape and neurite initiation are regulated by the Ndr kinase SAX-1, a member of the Orb6/COT-1/warts serine/threonine kinase family. Mol Biol Cell 11: 3177–3190.